euspen's 23rd International Conference & Exhibition, Copenhagen, DK, June 2023
www.euspen.eu

Study of auto-tuning of PID control parameter using PSO algorithm for active vibration isolation

Ilkyun An[1], Mijin Kim[1], Jaehyun Park[3], Kihyun Kim[2#], Hyo-Young Kim[2#]

[1] *Department of IT Semiconductor Engineering, Tech University of Korea, Republic of Korea*
[2] *Department of Mechatronics Engineering, Tech University of Korea, Republic of Korea*
[3] *Manufacturing System R&D Group, Korea Institute of Industrial Technology, Republic of Korea*

[#]Corresponding Autor / E-mail : kimhy@tukorea.ac.kr, [#]Co-Corresponding Author / E-mail : khkim12@tukorea.ac.kr

Abstract
PID control is a commonly used control method. Typical PID tuning methods, such as the Ziegler Nichols and pole placement methods, have the disadvantage of having to know the system model accurately or taking a lot of time due to manual repetitive tuning. Several auto-tuning methods have been studied to overcome these disadvantages. Optimization algorithms such as genetic algorithms are widely used for performing auto-tuning. In this study, we used the PSO algorithm, which an optimization algorithm, for the PID auto-tuning. The PSO algorithm has the advantage that its implementation is easy and has stable convergence performance. PSO consists of four processes: initialization, velocity calculation, location update, and evaluation. The objective function to be used for the evaluation was determined by comparing the four performance indicators commonly used in the control system: IAE, ISE, ITAE, and ITSE. To verify the performance of the PSO algorithm, simulations and experiments were performed by applying it to an active vibration isolator. Moreover, genetic algorithm was applied equally and was compared subsequently. The comparison confirmed that PSO-PID converges faster and has a better vibration isolation performance when compared to GA-PID.

PSO, auto-tuning, PID Control, active vibration Isolator

1. Introduction

Vibration isolation is a technology that reduces micro vibrations such as ground vibrations. Vibration isolation is typically used in precision processes such as precision measurements and in semiconductors. Because microvibration is directly related to product productivity, it is important to reduce the microvibration during the process[1-4]. Vibration isolation systems can be divided into two types: passive and active systems. Passive vibration isolation tables exhibit insufficient performance in the low-frequency range, and in recent years, active vibration isolation systems with actuators and sensors are used to overcome these weaknesses.

PID controllers have been used in many control systems because they are stable and easy to implement [5]. There are various PID tuning methods, such as the Ziegler Nichols and pole placement methods. However, these methods have the disadvantage that it consumes a significant amount of time for knowing the system model accurately. To overcome these disadvantages, several auto-tuning methods that uses optimization algorithms have been developed. As an experiment, a study on PID auto-tuning using genetic algorithm (GA) was conducted [6].

This paper proposes a method using the particle swarm optimization (PSO) algorithm, which is used for the auto-tuning of an active vibration isolator system. PSO is an algorithm that can be implemented using a simple structure and has a stable optimization performance with simple calculations. PSO consists of four processes: initialization, velocity calculation, location update, and evaluation. The objective function of PSO was selected by comparing four evaluation indicators (ISE, IAE, ITSE, and ITAE) that are commonly used in PID controllers. To verify the auto-tuning performance, a similar optimization algorithm, GA, was applied, which was thereafter compared and verified.

The remainder of this paper is organized as follows: Section 2 proposes the PSO-PID auto-tuning algorithm and performance index, Section 3 describes the modeling of the active vibration control system to which the proposed algorithm is applied, Section 4 compares and analyzes the simulation results, and Section 5 presents the conclusions of this study.

2. PSO algorithm

The PSO algorithm mimics social behavior patterns, such as birds and fish swarms in the ecosystem. In PSO, particles of position and velocity share information with each other in an N-dimensional search space, and simultaneously proceed with the optimization. The i^{th} N-dimensional particle can be expressed as $P_i = \{x_1, x_2, \ \ldots, \ x_N\}$, and the particle with the most optimal value is called *pbest*. The particle with the most optimal value during each iteration is called *gbest*. The velocity of each particle can be expressed $V_i = \{v_1, v_2, \ \ldots, \ v_N\}$ in the same way as the position. The PSO algorithm consists of four processes: initialization, speed calculation, location update, and evaluation for each iteration. The velocity calculation and position update are calculated as follows [7-9]:

$$\boldsymbol{v_{id}^{k+1} = w \cdot v_{id}^{k} + c_1 \cdot rand() \cdot (p_{id}^{k} - x_{id}^{k}) + c_2 \cdot rand() \cdot (p_{gd}^{k} - x_{id}^{k})} \tag{1}$$

$$\boldsymbol{x_{id}^{k+1} = x_{id}^{k} + v_{id}^{k+1}} \tag{2}$$

$$\boldsymbol{w = w_{max} - \frac{w\_\max - wmin}{G} \times i} \tag{3}$$

3. Active vibration isolator (AVI) modeling

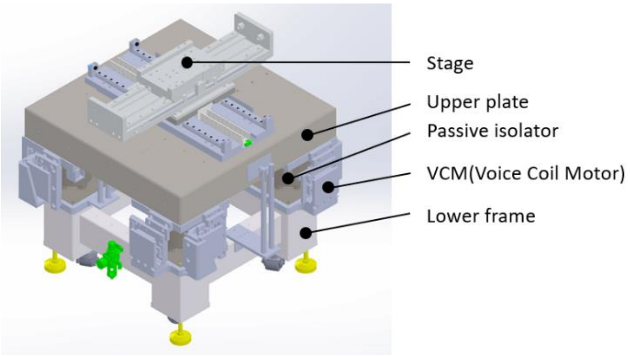

Figure 1. Configuration of active vibration isolation system

To control the 6-axis active vibration isolation system (AVIS) depicted in Figure 1, system modeling of the AVI is required. System modeling is the process of deriving an expression using differential equations.

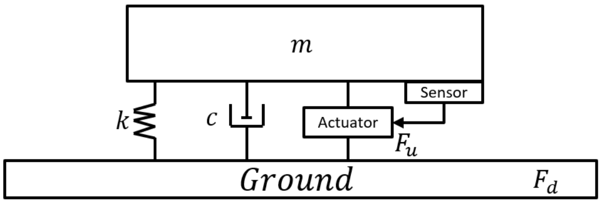

Figure 2. Modeling of active vibration isolator

For its application in the active vibration isolator, modeling was simplified and expressed as shown in Equation (4) and Figure 2 [10-12].

$$(ms^2 + cs + k)Z_p(s) = (cs + k)B(s) + F_u(s) + F_d(s) \quad (4)$$

The values of m, c, and k represent the mass, damping, and stiffness, respectively; $Z_p(s)$ represents the displacement in the z-axis direction; $B(s)$ represents the vibration from ground; $F_u(s)$ represents the actuator force; $F_d(s)$ represents the direct disturbance.

4. Simulation

4.1. Control algorithm

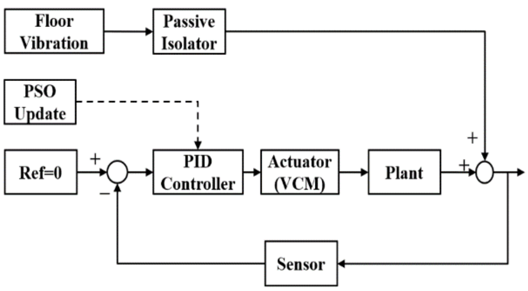

Figure 3. Block diagram of PSO

A control algorithm was created for conducting the simulation as depicted in Figure 3. Ground vibration is assumed to be disturbed by a passive vibration isolation module as it is transmitted through a lower frame, and the PID gain is updated based on the result value by applying the PSO's objective function to the error after receiving feedback from the sensor transfer function [13-17].

$$G_P = \frac{cs + k}{ms^2 + cs + k} \quad (5)$$

$$Transmissibility = \frac{G_p}{G_m * G_s * G_a * G_c + 1} \quad (6)$$

Equation (6) is a transfer function of the transmissibility to check the vibration-isolation performance. G_p represents the transfer function of the passive vibration isolation module, and G_m is the transfer function of the plant. G_s, G_a and G_c represent transfer functions of a sensor, actuator and controller.

4.2. Objective function

The smaller the average error, the faster the output of the system converges. Using this, the objective function of PSO was set to proceed with the simulation of the PSO algorithm. This study compared the integral of squared error (ISE), integral of absolute error (IAE), integral of time multiple squared error (ITSE), and integral of time multi absolute error (ITAE), which are primarily used in control system performance analysis. The error represents the difference between the reference value of the system and the output value, and is expressed by e.

$$ISE = \int_0^\infty e^2(t)dt \quad (7)$$

$$IAE = \int_0^\infty |e(t)|dt \quad (8)$$

$$ITSE = \int_0^\infty te^2(t)dt \quad (9)$$

$$ITAE = \int_0^\infty t|e(t)|dt \quad (10)$$

The PSO algorithm simulation was conducted by applying each objective function to analyze the effect of the characteristics of each method on the AVI.

Figure 4 depicts the results of the simulation to determine the objective function. All four objective functions demonstrated similar figures at maximum, whereas ITAE and ITSE, which gave weight to time, demonstrated a slow settling time. In addition, in the case of IAE and ISE, owing to their tendency to minimize errors, the P and I gains tended to converge to the maximum value rather than the appropriate value. To solve this problem, a simulation was carried out to obtain a fast settling time and an appropriate gain by adding a value weighted in the fixing time to the objective function. Equation (11) expresses the objective function with the settling time.

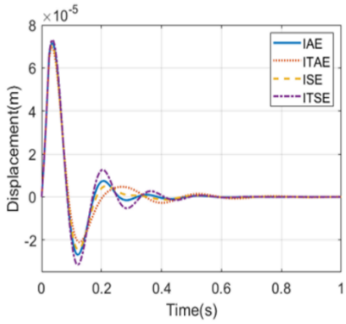

Figure 4. Performance of objective function

$$J = \int_0^\infty w_1|e(t)|dt + w_2 t_s \qquad (11)$$

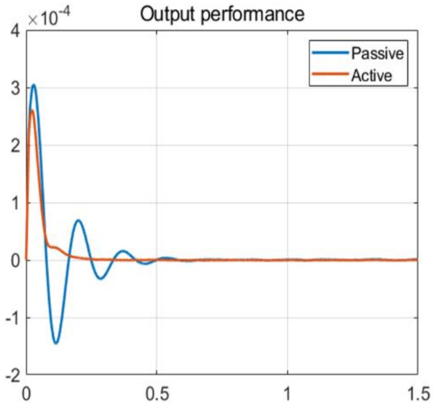

Figure 5. Result of objective function

Figure 5 depicts the simulation results obtained using Equation (11) as the objective function. The simulation shows that when the floor vibration is 100um, the settling time is 0.1798 seconds, which is controlled at a higher rate than when using existing objective functions.

4.3. Simulation result

Figures 6 and 7 depict the graphs of the best values of the objective function evaluation index for each iteration of PSO and GA, respectively. When comparing the two graphs, it was confirmed that PSO converges faster than GA and that the converging value is smaller when the same objective function is used.

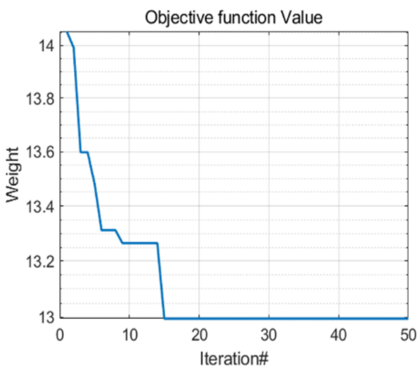

Figure 6. Objective function value of PSO

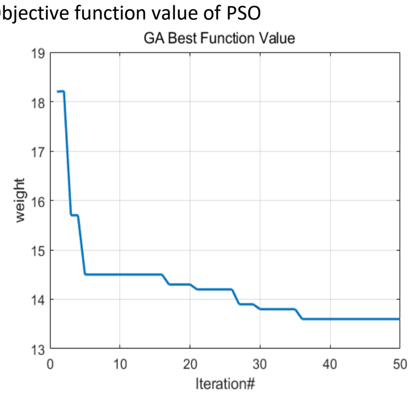

Figure 7. Objective function value of GA

Table1. Comparison of PSO and GA

	PSO	GA
Weight variation ratio	20%	25%
Iteration	15	36
P	100	85.26
I	47.23	46.82
D	0.03	3.13

Table 1 compares the PSO and GA graphs depicted in Figures 6 and 7, respectively. As a result of the comparison, the rate of change in the value of the objective function was smaller than that of the GA until the PSO converges; however, this is because the initial value of the objective function is lower than that of the GA. In the case of the convergence rate, the PSO was repeated 15 times and GA 36 times until the objective function value converged. When analyzing the above results and graphs, it was confirmed that PSO was superior to GA in terms of convergence speed, although the performance of the gain-tuning values of the two algorithms was not significantly different.

Figure 8 depicts the transmissibility in the frequency response using Equation (6). While observing the 8 Hz band, which is the resonance frequency of the vibration isolator, it can be seen that the performance of active vibration isolation decreases by -10 dB or more compared to passive vibration isolation and thereafter, improves.

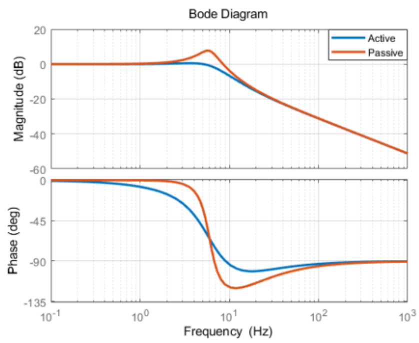

Figure 8. Bode-plot of PSO-PID

5. Experiment

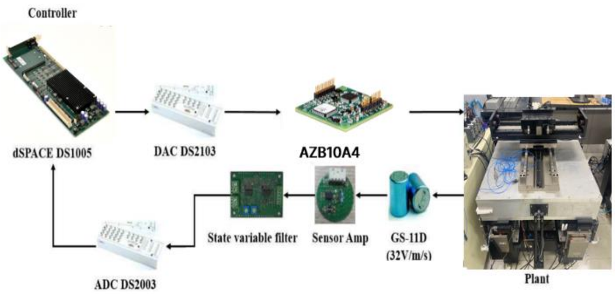

Figure 9. Configuration of experiment

The tendency to follow the reference input according to the control state was analyzed after applying a direct disturbance to the actual vibration control system as depicted in Figure 9. In the

PID gain, the P, I, and D values obtained through PSO were registered, and an experiment was conducted. The results of the experiment are depicted in Figure 10.

As a result of applying direct disturbance to the vibration isolator, it was confirmed that the peak value and settling time did not differ significantly from the passive state. This is because there was no significant difference before and after the control by directly applying a force to the upper mass. Therefore, the performance should be evaluated by measuring the transmissibility before and after the control.

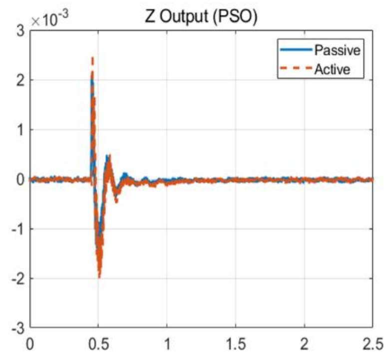

Figure 10. Ouput of z-axis

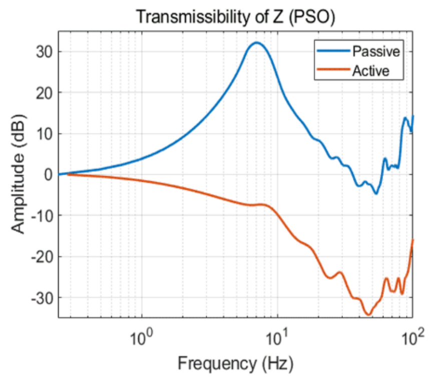

Figure 11. Transmissibility of z-axis

A transmissibility measurement experiment was conducted to evaluate the vibration isolation performance. To measure the transmissibility, an accelerometer was attached to the upper mass of the vibration isolator and center of the ground. Subsequently, the impact was applied to the ground to determine the ratio of the measured physical amount. The measured physical quantity was calculated after converting into the frequency domain using a fast Fourier transform (FFT). The results of the transfer-rate measurements are depicted in Figure 11. The measurement results demonstrated an improvement of approximately -40 dB in the resonant frequency 8 Hz band.

6. Conclusion

To evaluate the performance of the PSO, the same parameters were applied to the GA, compared, and analyzed. Simulation results demonstrated that the PSO and GA have similar control performance; however, PSO has a faster convergence rate when compared to GA. In addition, it was confirmed that the resonance frequency improved by approximately -10 dB when the control simulation was performed by applying the gain value obtained from the PSO. The experiment was conducted by applying the gain value derived from the simulation to an actual system. Control performance experiments were conducted by applying direct disturbance to the upper part of the vibration isolator. As a result of the experiment, the difference before and after the control was not significant; therefore, a vibration control experiment was conducted. For the vibration control experiment, an accelerometer was placed at the upper mass of the vibration isolator and at the center of the ground to measure the transmissibility. As a result of the measurement, it was confirmed that in the case of PSO, approximately the resonance frequency improved by -40 dB.

Acknowledgement

This work was supported by Korea Institute for Advancement of Technology (KIAT) grant funded by the Korea Government (MOTIE) (P0021527, P0008458), and GRRC programme of Gyeong-gi province [(GRRC TU Korea2020-B02). This work was supported by the Korea Evaluation Institute of Industrial Technology (20017202,KM230031) funded By the Ministry of Trade, Industry & Energy(MOTIE, Korea)

References

[1] Kim K H, LEE H and Ho 2018 Vibration Isolation and Reaction Force Compensation for a Precision Positioning system Korea Polytechnic University

[2] Kim K H and Choi J S 2020 Study on an Active Vibration Isolation with respect to inertia variations Korea Polytechnic University

[3] Kim B S and Kim K W 2018 Cooling Analysis of Super Precision and Large Stage for OLED *Journal of the Semiconductor & Display Technology* **17(4)** 51-55

[4] An C H, Choi J H, Park J S and Park M S 2021 A Review of Experimental Evaluation Method to Floor Environment Vibration Criteria for Semiconductor and Display Equipment *Journal of the Semiconductor & Display Technology* **20(1)** 25-31

[5] Ou C and Lin W 2006 Comparison between PSO and GA for parameters optimization of PID controller *In 2006 International conference on mechatronics and automation* 2471-2475 IEEE

[6] Fan L, and Joo E M 2009Design for auto-tuning PID controller based on genetic algorithms *In 2009 4th IEEE Conference on Industrial Electronics and Applications* 1924-1928 IEEE

[7] Solihin M I, Tack L F and Kean M L 2011Tuning of PID controller using particle swarm optimization (PSO) *In Proceeding of the international conference on advanced science, engineering and information technology* **1** 458-461

[8] Kennedy J, and Eberhart R 1995Particle swarm optimization *In Proceedings of ICNN'95-international conference on neural networks* **4**1942-1948) IEEE

[9] Shi Y, and Eberhart R 1998 A modified particle swarm optimizer *In 1998 IEEE international conference on evolutionary computation proceedings* IEEE world congress on computational intelligence (Cat. No. 98TH8360) 69-73) IEEE

[10] Lee J H, Kim H Y, Kim K H, Kim M H and Lee S W 2017 Control of a hybrid active-passive vibration isolation system *Journal of Mechanical Science and Technology* **31(12)** 5711-5719

[11] Liu C, Jing X, Daley S and Li F 2015 Recent advances in micro-vibration isolation *Mechanical Systems and Signal Processing* **56** 55-80

[12] Kim M H, Kim H Y, Kim H C, Ahn D and Gweon D G 2016 Design and control of a 6-DOF active vibration isolation system using a Halbach magnet array *IEEE/ASME Transactions on Mechatronics* **21**(4) 2185-2196

[13] Liu Y, Matsuhisa H and Utsuno H 2008 Semi-active vibration isolation system with variable stiffness and damping control *Journal of sound and vibration* **313(1-2)** 16-28

[14] Pérez-Aracil J, Pereira E, Díaz I M and Reynolds P 2021 Passive and active vibration isolation under isolator-structure interaction: application to vertical excitations *Meccanica* **56**(8) 1921-1935

[15] Fu Y, Li S, Liu J and Zhao B 2021 Design and Experimentation of a Self-Sensing Actuator for Active Vibration Isolation System with Adjustable Anti-Resonance Frequency Controller *Sensors*, **21**(6) 1941

[16] Mohamad M, Mailah M and Muhaimin A H 2004. Vibration control of mechanical suspension system using active force control (Doctoral dissertation, Universiti Teknologi Malaysia)

[17] Mayer D, and Herold S 2018 Passive, Adaptive, Active Vibration Control, and Integrated Approaches. Vibration Analysis and Control in Mechanical Structures and Wind Energy Conversion Systems, 1